Comparing crystal–melt interfacial free energies through homogeneous nucleation rates

2008 J. Phys.: Condens. Matter 20 375103

(http://iopscience.iop.org/0953-8984/20/37/375103)

J. Phys.: Condens. Matter **20** (2008) 375103 (7pp) doi:10.1088/0953-8984/20/37/375103

Comparing crystal–melt interfacial free energies through homogeneous nucleation rates

Xian-Ming Bai[1] **and Mo Li**[2]

School of Materials Science and Engineering, Georgia Institute of Technology, Atlanta, GA 30332-0245, USA

E-mail: xmbai@northwestern.edu and mo.li@mse.gatech.edu

Received 27 June 2008, in final form 27 July 2008
Published 26 August 2008
Online at stacks.iop.org/JPhysCM/20/375103

Abstract

In this work, we compared several available crystal–melt interfacial free energies via homogeneous nucleation rates in a pure Lennard-Jones model system using both model fitting and numerical methods. We examined the homogeneous nucleation temperature obtained from the classical nucleation theory using the available interfacial free energies from three different methods as inputs, i.e. the free energy integration method, the interface fluctuation method and the classical nucleation theory based method. We found that the critical temperature obtained by using the interfacial free energy calculated recently (Bai and Li 2006 *J. Chem. Phys.* **124** 124707) is in better agreement with that obtained from spontaneous crystallization in an independent molecular dynamics simulation. The discrepancies among the interface energies are discussed in light of these results.

(Some figures in this article are in colour only in the electronic version)

1. Introduction

The crystal–melt interfacial free energy is an important physical quantity for solid–liquid phase transitions. It is directly related to the nucleation kinetics and crystal-growth morphologies [1]. However, unlike liquid–vapor and solid–vapor interfaces that are accessible easily in experiments, the crystal–melt interface is inherently difficult to obtain as it lies between two condensed phases (i.e. solid and liquid phases) [2, 3]. Moreover, the crystal–melt interfacial free energy is very weak. Generally, its magnitude is only several tens of millijoules per square meter for most metals [1]. Therefore, it is difficult to accurately determine the crystal–melt interfacial free energy experimentally. Turnbull and coworkers [4, 5] developed an experimental method to extract the crystal–melt interfacial free energy from homogeneous nucleation rates. Based on the experimental results, Turnbull proposed an empirical relation between the interfacial free energy and the latent heat of fusion [6]:

$$\gamma_{SL} = \alpha \rho^{2/3} (\Delta H_f / N_a), \tag{1}$$

where γ_{SL} is the solid–liquid (or crystal–melt) interfacial free energy, α is a coefficient whose value is 0.45 for most metals and 0.32 for most nonmetals, ρ is the atom number density of the crystal, ΔH_f is the gram atomic heat of fusion, N_a is Avogadro's number and thus $\Delta H_f / N_a$ is the enthalpy per atom. Although in this method [4, 5] the heterogeneous nucleation can be suppressed to a large degree, the catalysts (e.g. container walls, impurities, etc) could still play significant roles in affecting the homogeneous nucleation rates [6]. More advanced methods such as containerless processing [7] have been developed recently. Although the heterogeneous nucleation can be suppressed further with these advanced techniques, it is still difficult to obtain the melt–crystal interface free energy accurately.

An alternative way to obtain the crystal–melt interfacial free energy is to use computer simulations in which catalyst effects can be ruled out completely. Over the past twenty years, different methods [8–15] have been developed. Broughton and Gilmer [8] devised a free energy integration scheme to

[1] Present address: Department of Chemical and Biological Engineering, Northwestern University, Evanston, IL 60208-3120, USA.

[2] Author to whom any correspondence should be addressed.

Table 1. The solid–liquid interfacial free energies (in units of ε/σ^2) calculated with different methods for a standard Lennard-Jones model system. The estimated errors in the last digits are indicated by the numbers in parentheses. (Note: LJ: Lennard-Jones; HD: hard-sphere).

	Method	$\gamma_{SL}^2/\varepsilon$
Morris and Song [13]	Interface fluctuation method (LJ)	0.362(8)[a]
Davidchack and Laird [10]	Reversible work integration (HD, cleaving walls)	0.360(1)[a]
Broughton and Gilmer [8]	Reversible work integration (LJ, cleaving potential)	0.350(2)[a]
Davidchack and Laird [26]	Reversible work integration (HD, cleaving walls, recent work)	0.334(3)[a]
Davidchack *et al* [17]	Interface fluctuation method (HD, recent work)	0.326(10)[a]
Turnbull [6]	Empirical estimation from experiments (equation (1))	0.330[b]
Bai and Li [15]	Classical nucleation theory based approach (LJ)	0.302(2)

[a] The interfacial free energy is approximated by taken the simple arithmetic mean over (100), (110) and (111) orientations. More accurate values can be calculated by using the expressions in [17] because the values for three orientations do not have the equal weight for the calculation of the orientationally averaged interfacial free energy.

[b] For nonmetals, the interfacial energies can be expressed empirically as $\gamma_{sl} = 0.32\Delta L_n \rho_s^{2/3}$ [6]. For a Lennard-Jones system, $\Delta L_n = 1.075\varepsilon$ is the latent heat per atom and $\rho_s = 0.94/\sigma^3$ is the number density of the crystal [15].

calculate the crystal–melt interfacial free energies of different crystallographic interface planes directly. They applied an external 'cleaving potential' to join a bulk crystal and a bulk liquid and calculated the reversible work in this process. The 'cleaving potential' was chosen carefully to make the combination process reversible. Davidchack and Laird [9, 10] extended this method by introducing two cleaving walls for both hard-sphere [9] and Lennard-Jones [10] systems. In order to avoid the inconvenience of choosing the reversible path, Mu and Song [11] used a multistep thermodynamic perturbation method in which the exact reversible path is no longer needed. However, the path cannot be chosen arbitrarily and still needs to be close to the reversible path in order to achieve convergence. Hoyt *et al* [12] developed an interface fluctuation method or capillary fluctuation method to calculate the anisotropic interfacial free energies from the fluctuations of rough crystal–melt interfaces. This method has been tested in embedded-atom-method (EAM) [12, 16], Lennard-Jones (LJ) [13], hard-sphere [17] and molecular [18] systems. Different from the aforementioned methods in which the simulations need to be performed at the equilibrium melting temperature with a planar interface, the present authors [14, 15] developed a method based on the classical nucleation theory with a curved interface to calculate the crystal–melt interfacial free energy. In our method, we 'inserted' spherical crystalline nuclei of various sizes into an undercooled liquid and determined their (unstable) coexistence temperatures. The interfacial free energy was extracted by fitting the relation between the critical nucleus size and the critical undercooling. This method therefore produces the interfacial free energy averaged over all orientations and a wide range of undercooling temperatures. In other words, the information of the anisotropy in the interface free energy is lost. However, this problem may be rectified by using faceted nuclei with specific crystallographic planes on the interface [19, 20]. As we discuss later in this paper, clearly, the use of spherical nuclei is an approximation because the spontaneously formed crystal nuclei in simulations [21] and experiments [22] are found to be nonspherical and the nucleus surface is very rough at deep undercooling. Thus, the ramified morphologies of the nuclei may challenge the assumption. At shallow or moderate undercooling, most nuclei formed in the LJ systems do not have ramified geometries [23]. To put it differently, the nuclei seldom have rod-like or disc-like shapes. In addition, the anisotropy in the interfacial free energy in a Lennard-Jones model system is shown to be very weak [8, 10, 13] and the contribution from the datum points obtained at the deep undercooling is limited. Therefore, the variation of the interfacial free energy caused by the ramified nucleus morphologies at deep undercooling is expected to be small. For these reasons and for the lack of any effective ways to treat the nuclei with stochastically varying shapes and sizes, the assumption of spherical nuclei is still a reasonable approximation. In the past, classical nucleation theory has been used widely and successfully for analyzing nucleation [21, 22, 24, 25]. We shall stick to this approximation in the rest of this work.

The crystal–melt interfacial free energies calculated via different methods in a standard LJ system or a hard-sphere system are shown in table 1. All the interfacial energies are converted to the values in LJ unit. Note that the interfacial free energies shown in the first five rows are the average values (arithmetic means) over (100), (110) and (111) crystallographic planes. Turnbull's experimental estimation (equation (1)) is also shown for comparison. The value obtained by Turnbull has been used extensively in the past to validate the theoretical calculations [8–15]. The tabulated data show a wide variation. If we consider Turnbull's experimental estimation as a 'standard' reference, we can see that the interface free energies obtained from the free energy integration method and the interface fluctuation method (the first three rows in table 1) are about 9% larger than Turnbull's value, whereas our result is about 9% smaller, or the lowest among the available data. The difference in the interfacial free energy obtained from different approaches is large enough to warrant an in-depth consideration. (We shall mention in passing that recently Davidchack *et al* have used an improved reversible work integration method [17] and interface fluctuation method [26] to re-calculate the crystal–melt interfacial free energies in hard-sphere systems (the fourth and fifth rows in table 1). Also the new results are about

7%–10% smaller than their previous values and are very close to Turnbull's estimation.)

There has not been any 'first principles' approach or direct way that could give an exact value for the interfacial free energy. In order to examine the origin of the discrepancy among these results, we have to use indirect ways. One way is via a homogeneous nucleation rate, as Turnbull did in his famous experiment [4, 5]. As shown below, the difference among the interfacial free energies can be observed very sensitively through the crystallization nucleation rate. In this paper, we shall address the difference through the connection between the interface free energy and the homogeneous nucleation rate.

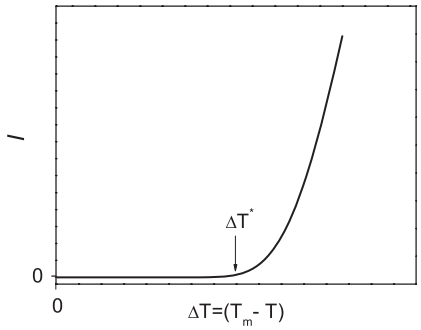

Figure 1. Schematic illustration of the relation between the homogeneous nucleation rate (I) and undercooling (ΔT). ΔT^* represents the critical undercooling for the onset of homogeneous nucleation [1].

2. Theory and modeling fitting

According to classical nucleation theory (CNT) [1], the homogeneous nucleation rate is expressed as

$$I = I_0 \exp(-\Delta G^*_{\text{hom}}/k_{\text{B}}T), \tag{2}$$

where I_0 is a prefactor [4–6, 27] of the order of 10^{32-33} cm^{-3} s^{-1} and ΔG^*_{hom} is the homogeneous nucleation barrier. In classical nucleation theory, ΔG^*_{hom} can be calculated through the following relation [1]:

$$\Delta G^*_{\text{hom}} = \left(\frac{16\pi\gamma^3_{\text{SL}}T^2_{\text{m}}}{3L^2_V}\right)\frac{1}{(\Delta T)^2}. \tag{3}$$

In equation (3), T_{m} is the equilibrium melting temperature at which a bulk solid and a bulk liquid coexist with a flat interface, L_V is the latent heat per volume and $\Delta T = T_{\text{m}} - T (T \leqslant T_{\text{m}})$ is the undercooling. Equations (2) and (3) show that the nucleation rate is related to the undercooling temperature exponentially, as shown in figure 1 [1]. When the temperature is high (or the undercooling is small), the nucleation rate is almost zero. But as ΔT approaches the critical undercooling ΔT^*, the nucleation rate increases very rapidly. The temperature corresponding to the rapid change in nucleation rate, as shown in figure 1, marks the onset of homogeneous nucleation. For convenience, we define this critical temperature as a spontaneous nucleation/crystallization temperature in a homogeneous nucleation. How to determine ΔT^* operationally will be discussed shortly.

On the other hand, the nucleation rate is related sensitively to the interfacial free energy as the nucleation rate varies exponentially with γ^3_{SL} (equation (3)), or

$$I = I_0 \exp[-A(T)\gamma^3_{\text{SL}}], \tag{4}$$

where $A(T) = (\frac{16\pi T^2_{\text{m}}}{3L^2_V})\frac{1}{k_{\text{B}}T(T_{\text{m}}-T)^2}$ is a function of the temperature T. Therefore, a slight variation of γ_{SL} can change the nucleation rate significantly. In other words, the relation between the nucleation rate and the interfacial free energy can be used to examine the different interface free energies calculated using the aforementioned methods. Note that CNT may not be valid for some real material systems nor under very deep undercooling [23]. In this work, we simply invoke this approach to make comparisons among the interface energies in a self-consistent way.

To this end, first we used some interfacial free energies listed in table 1 as inputs for equation (4) to estimate the respective homogeneous nucleation temperatures. The results are shown in figure 2(a). To make it representative, we choose three interfacial free energies as inputs: our calculated value of 0.30 ε/σ^2, Turnbull's empirical estimation of 0.33 ε/σ^2 and a value of 0.36 ε/σ^2 which is typical for the others' methods, where ε and σ are the LJ parameters to be explained below. For an LJ system, we use $L_V = 1.024\ \varepsilon/\sigma^3$ and $T_{\text{m}} = 0.618\ \varepsilon/k_{\text{B}}$ at zero external pressure [15]. From equation (4) and three representative interface free energies, we calculated the respective nucleation rates as a function of temperature (figure 2(a)). From figure 2(a), one can find that the different interfacial free energies yield quite different nucleation rates. Apparently, the predicted nucleation rate at deep undercooling, using the interfacial free energy calculated through a planar interface (denoted as the others' method), is several orders of magnitude smaller than Turnbull's experimental result. This is in good agreement with Baez and Clancy's work [28] in which they also found that, using the interfacial free energy obtained from a planar interface, the predicted nucleation cluster populations were underestimated to several orders of magnitude. In passing, we should mention that the estimated nucleation rates in figure 2(a) are normalized values (i.e. I/I_0).

In order to give more quantitative assessment for the differences in the interfacial free energies, we need to have an estimate of the critical nucleation rate or critical value of I/I_0 at spontaneous nucleation. In the following, we give a simple argument for the critical nucleation rate. Aga *et al* [29] measured the nucleation time and number of critical nuclei at deep undercooling for aluminum. In the second figure of their work, the nucleation time is about 50 ps (taken from the well-fitted Shi *et al*'s theoretical curve [30]) and the number of nuclei is about 4 for a system consisting of 16 384 atoms (or $16 \times 16 \times 16$ unit cells) at deep undercooling ($T = 500$ K, $\Delta T/T_{\text{m}} = 0.47$). Since the aluminum lattice constant is about 0.405 nm, the box length of the simulation system is 6.48 nm. Therefore, the nucleation rate is $4/50$ ps/(6.48 nm)$^3 = 294 \times (10\text{ nm})^{-3}$ ns^{-1} in their work, meaning that there are 294 critical nuclei in a

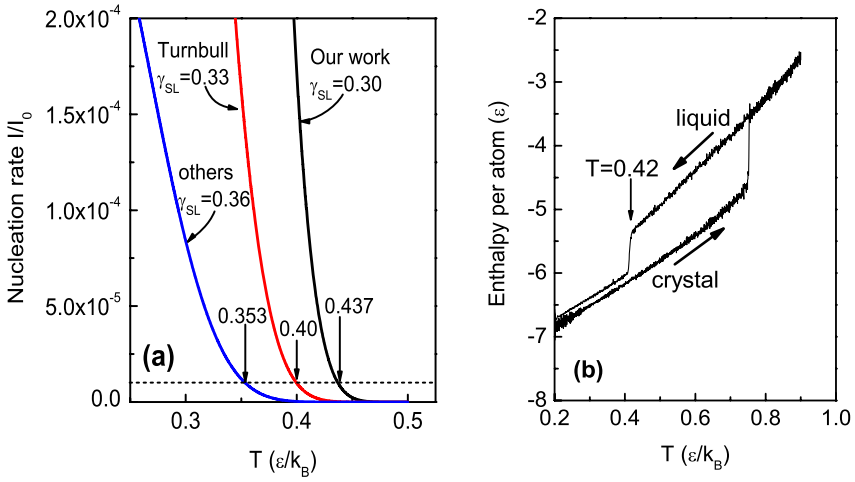

Figure 2. (a) The theoretical prediction of the nucleation rates (equation (4)) with different interfacial free energies as inputs. The dashed line indicates the critical nucleation rate, $I/I_0 = 10^{-5}$ or $I = 1 \times (10\ \text{nm})^{-3}\ \text{ns}^{-1}$. The arrows indicate the corresponding homogeneous nucleation temperatures with different interfacial free energies as inputs. (b) The hysteresis loop of the enthalpy in the heating–cooling process. The cooling rate is 3.33×10^9 K s^{-1} and the system has 2048 atoms. The arrow indicates the spontaneous crystallization temperature of the pure liquid.

simulation box of 10 nm^3 per nanosecond (ns). This is the typical observable nucleation rate in MD simulation. In our work, we take the commonly used prefactor [27] from the classical nucleation theory, $I_0 = 10^{32}\ \text{cm}^{-3}\ \text{s}^{-1}$. If we choose $I/I_0 = 10^{-5}$, the corresponding nucleation rate is about $I = 10^{27}\ \text{cm}^{-3}\ \text{s}^{-1} = 1 \times (10\ \text{nm})^{-3}\ \text{ns}^{-1}$, which is one critical nucleus in a simulation box of 10 nm^3 per nanosecond (ns). This nucleation rate is already about 300 times lower than that in Aga *et al*'s work [29]. Thus, it is reasonable to use this value to define the critical spontaneous nucleation rate. Of course one can choose an even lower nucleation rate such as $I/I_0 = 10^{-7}$, but it is doubtful that massive nucleation can take place at such low nucleation rate, not to mention whether such a low probability event is observable in either experiments or computer simulations. Therefore, in this work we use $I/I_0 = 10^{-5}$ as the threshold for the nucleation rate.

Using this nucleation rate as a reference value (the dashed line in figure 2(a)), we estimated that the spontaneous nucleation temperature should be about 0.437 ε/k_B (or $0.71T_\text{m}$) for the interfacial free energy from our earlier calculation, 0.40 ε/k_B (or $0.65T_\text{m}$) for Turnbull's estimated value and about 0.353 ε/k_B (or $0.57T_\text{m}$) for the other methods. For comparison, we also took a lower bound at $I/I_0 = 10^{-6}$. The spontaneous nucleation temperature is about 0.456 ε/k_B (or $0.74T_\text{m}$), 0.425 ε/k_B (or $0.69T_\text{m}$) and 0.387 ε/k_B (or $0.63T_\text{m}$) for the corresponding interfacial energies, respectively.

3. Simulation method

To test the above results estimated from the model fitting, independent verification with model-free approaches must be conducted. To this end, we employed molecular dynamics (MD) simulations to determine the spontaneous (homogeneous) crystallization temperature during the process of cooling a pure LJ liquid. The crystallization in this test occurs homogeneously as there are no heterogeneous nucleation sites in the simulation system.

In the MD simulation, first we arranged 2048 solid argon atoms in an fcc lattice with the equilibrium lattice parameter at the temperature $T = 24$ K. Then we heated the system from this temperature to a high temperature (108 K). The crystal sample becomes a liquid during the heating process. We held the sample at this temperature for some time to obtain a fully equilibrated liquid before we cooled the liquid slowly from the highest temperature to the initial temperature which is below the equilibrium melting point (74.2 K). During the cooling process, the undercooled liquid starts to crystallize at the spontaneous crystallization temperature. The detailed description of the heating–cooling process and its effect on the nucleation is given in section 4.

The interatomic potential used in the simulation is a standard Lennard-Jones potential, $\phi(r) = 4\varepsilon[(\sigma/r)^{12} - (\sigma/r)^6]$, where $\varepsilon/k_\text{B} = 119.8$ K and $\sigma = 3.405$ Å. The cutoff distance was set to 2.5 σ. In some previous work [10, 13], a continuous function was used to make the LJ potential approach zero smoothly at the cutoff distance. We used this potential in an independent simulation to obtain the bulk properties. We found that the difference in the latent heat obtained from two potentials is negligible. To suppress the free surface effects, periodic boundary conditions were applied in all three Cartesian directions. The simulation was performed in an isothermal–isobaric ensemble (i.e. an *NPT* ensemble, where N is the number of particles, P is the external pressure and T is the system temperature). In this ensemble, the Parrinello–Rahman method [31] was used to maintain zero external pressure and adjust the system volume at different temperatures. A velocity rescaling method [32] was used to control the system temperature at every MD step. The MD time step was set to 5×10^{-15} s. In order to be consistent with the existing literature data, the standard reduced LJ units [33] were used in this work: the mass unit was set as the weight of

one argon atom m, length unit in σ, energy unit in ε, time unit in $\tau = \sqrt{m\sigma^2/\varepsilon}$, temperature unit in ε/k_B and the interfacial free energy unit in ε/σ^2.

4. Results and discussion

Figure 2(b) shows the heating and cooling process in our MD simulation and the anticipated homogeneous crystallization. First we equilibrated the crystal system at the temperature of 0.2 ε/k_B (24 K) for 10 000 MD steps. Then we heated the crystal from this temperature with an increment of 1.667×10^{-3} ε/k_B (or 0.2 K) every 300 MD steps (or 1.5×10^{-12} s). So the heating rate is 1.33×10^{11} K s^{-1}. The enthalpy of the system (per atom) increases with increasing temperature. At $T = 0.75$ (90 K), the system enthalpy has an abrupt jump, indicating melting. This temperature is called the upper superheating limit as the melting occurs at a higher temperature above the normal melting point (0.618) due to the absence of free surface in the system [15]. To have a homogeneous liquid, the system was heated further to 0.9 (108 K). After the system was equilibrated for another 10 000 MD steps at this temperature, it was cooled down to the initial temperature 0.2 with a decrement of 4.167×10^{-4} ε/k_B (or 0.05 K) every 3000 MD steps (or 1.5×10^{-11} s) or a cooling rate of 3.33×10^9 K s^{-1}. In the cooling process, the system enthalpy decreases with decreasing temperature. Since the system is still in the liquid state, the liquid enthalpy is higher than that in the crystal state at the same temperature. At around $T = 0.42$, the system enthalpy starts to decrease rapidly and approaches the crystal enthalpy, indicating that homogeneous crystallization takes place at this temperature. The onset temperature at the change of the enthalpy is determined as the spontaneous crystallization temperature.

From the results we can see that the spontaneous crystallization temperature obtained from freezing the LJ liquid (0.42) is close to the theoretical prediction (0.437) using equation (4) with our calculated interfacial free energy as the input, whereas it is much higher than the predicted value (0.353) using the others' calculated interfacial free energy as the input. Furthermore, the predicted temperature using Turnbull's empirically estimated interfacial free energy (0.40) is also close to the transition temperature obtained from the simulation. These results indicate that practically using the interface free energy obtained from our method as well as from Turnbull's estimation one can get the spontaneous crystallization temperatures close to that obtained from the independent freezing simulation, while using the interfacial free energy obtained from the others' methods one predicts a lower transition temperature.

The difference in the interfacial free energies among different methods may be attributed to the following causes. First, according to the Ostwald rule of stages [34], two or three surface layers of an fcc crystal nucleus may form a metastable structure (e.g. bcc-like [35], random hcp [21], or hybrid fcc and hcp [36]) first before they transform to a stable fcc structure later during the crystal growth. For instance, the bcc structure has been verified as the precursor to fcc crystal growth in both experiments [37] and computer simulations [35, 38]. Independent calculations show that, even for the same system, the bcc–melt interfacial free energy is about 20%–35% smaller than the fcc–melt interfacial free energy [16, 26, 39]. For other metastable structures (of lower energy barriers), we also expect similar interfacial free energy reduction. At deep undercooling, the nucleus size is very small (typically consisting of fewer than 100 atoms) and the surface to volume ratio is very high. If the surface layers of a crystal nucleus are dominated by metastable structures, it is reasonable to expect the crystal–melt interfacial energy of a small nucleus is lower than that for a planar interface. Second, at deep undercooling, there may be the so-called spinodal effect, which could lead to smaller interface energy [23, 40–42]. Computer simulations [23, 41, 42] and mean-field theory [40] have shown that, at shallow or moderate undercooling, the crystallization process follows the classical nucleation picture (i.e. the nucleation-growth mechanism). The spontaneously formed nuclei have near-spherical or ellipsoidal geometries [23, 41]. Deep quenching, however, may lead to the critical droplets with ramified (nonspherical) geometries and spatially diffusive (non-compact) nature in the interfaces [23, 41]. Third, it was found that in both experiments [43–45] and simulations [15] the crystal–melt interfacial free energy increases with increasing temperature. Given the fact that our simulations were performed in a wide range of supercooled temperatures below the melting point, while the others' simulations were performed at the equilibrium melting temperature, it is reasonable to expect that their values are higher. For example, by using the temperature-dependent latent heat as done by other researchers [29], we have found that our interfacial free energy increases to 0.315 ε/σ^2 at the equilibrium melting temperature [15]. Fourth, according to Tolman [46], the interfacial free energy is curvature-dependent [47, 48]. In our method, we used spherical nuclei in a supercooled liquid. Thus, the calculated interfacial free energy is for curved interfaces, which is more relevant to homogeneous nucleation at the actual critical undercooling. As we mentioned before, Baez and Clancy [28] also found that the interfacial free energy calculated from a planar interface fails to predict the nucleation rate (of curved nuclei) at deep undercooling. Due to these reasons, it is reasonable to see why our interfacial free energy should be smaller than the others'. Note that this does not mean our method is more accurate in the interface energy calculation than the others' methods. At high temperatures such as the melting point, the interfacial free energy calculated from the others' methods may be more accurate. However, at low temperatures such as deep undercooling, we think that the interfacial free energy calculated from a planar interface should be adjusted to a smaller value in order to correctly fit the spontaneous nucleation rate. This conclusion is supported by our results and the others' work including Aga *et al*'s recent work [29] in which they found the crystal–melt interfacial free energy obtained from the interface fluctuation method should be lowered to about 20% from the original value in order to fit the nucleation rates obtained directly from the homogeneous nucleation simulations. Fifth, the simulation ensemble used in our work is an NPT ensemble. In this ensemble, the

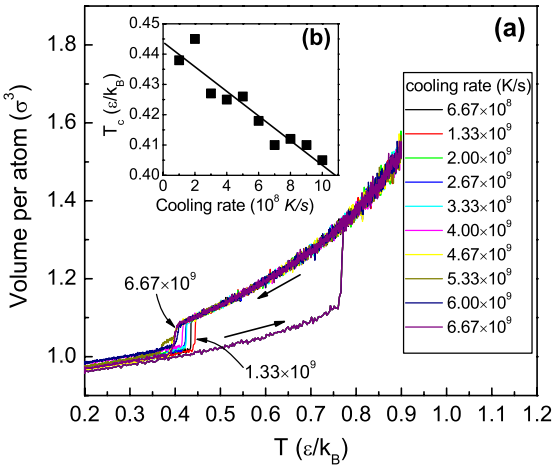

Figure 3. Cooling rate dependence on the spontaneous crystallization temperature. The number of atoms in these simulations is 2048. (a) The hysteresis loops of the volume per atom in the heating–cooling process at ten different cooling rates. (b) The spontaneous crystallization temperature (T_c) as a function of the cooling rate for the same size system.

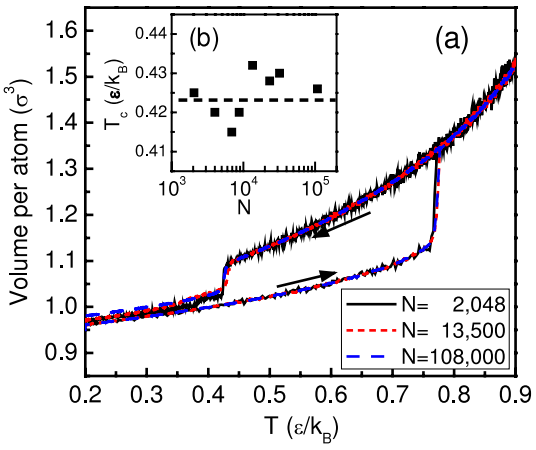

Figure 4. Size dependence on the spontaneous crystallization temperature. The cooling rate in these simulations is 3.33×10^9 K s^{-1}. (a) The heating–cooling hysteresis loops of three different size systems. (b) The spontaneous crystallization temperature (T_c) as a function of the system size at the same cooling rate.

system temperature, volume and pressure are well controlled at the desired conditions, which may not be easily controlled in other ensembles of finite sizes. As a result, some errors could be introduced because the crystal–melt interfacial free energy is very weak. Finally, different approaches have their own systematic errors and approximations. For example, Davidchack and coworkers [17, 26] have revisited their interfacial energy calculation with more accurate control of parameters and found the new results [17, 26] are about 10% lower than their previous values [9, 10] obtained from the same methods. As shown in table 1, their recent results are very close to Turnbull's experimental estimation.

Next, we shall address the cooling rate and finite system size effects in the MD simulation. In order to check the cooling rate dependence, we fixed the system size at 2048 atoms and used different cooling rates in our simulations. Figure 3(a) shows the heating–cooling processes at ten different cooling rates ranging from 6.67×10^8 to 6.67×10^9 K s^{-1} with an increment of 6.67×10^8 K s^{-1}. For the fastest cooling rate of 6.67×10^9 K s^{-1}, we decreased the system temperature of $8.333 \times 10^{-4} \varepsilon/k_B$ (or 0.1 K) every 3000 MD steps (or 1.5×10^{-11} s), and for the slowest cooling rate of 6.67×10^8 K s^{-1}, we decreased the system temperature of 8.333×10^{-5} ε/k_B (or 0.01 K) every 3000 MD steps (or 1.5×10^{-11} s). We found that the spontaneous crystallization temperature increases with decreasing cooling rate: if the cooling rate is 6.67×10^9 K s^{-1} (fastest), the transition temperature is at 0.405; if the cooling rate is 6.67×10^8 K s^{-1} (slowest), the transition temperature is at 0.435. At each cooling rate, we determined a corresponding spontaneous crystallization temperature. Figure 3(b) shows the transition temperature as a function of the cooling rate. Although the cooling rate dependence shows some variations, in general the transition temperature varies almost linearly in the range from 0.40 to 0.45, which is well within the range of the predictions from equation (4) using our result and Turnbull's empirical estimation (also Davidchack *et al*'s recent results [17]) as inputs. On the other hand, the homogeneous nucleation temperature obtained using the others' result as input is outside of this range. It is worth mentioning that, in our simulations, the slowest cooling rate is 6.67×10^8 K s^{-1}, which requires about 30 million MD steps for completing a single cooling process. It almost reaches the limit of our computing capacity. However, this cooling rate is still much faster than the usual cooling rate in a real experiment. Thus, it is reasonable to predict that the transition temperature may further increase with the decreasing cooling rate. If this is true, the interfacial free energy may be even smaller than our result (note our result is the smallest among different methods). However, we are unable to predict whether the transition temperature would keep increasing linearly or approaches a saturated value eventually. More investigations are needed to determine the trend of the spontaneous crystallization temperature as a function of the cooling rate in the future.

Finally, in order to check the finite-size effect, we fixed the cooling rate at 3.33×10^9 K s^{-1} and tested ten different system sizes ranging from 2048 to 108 000 atoms, as shown in figure 4. For the sake of clarity, only the results of three representative size systems are shown in figure 4(a): 2048, 13 500 and 108 000. The spontaneous crystallization temperature only varies slightly even if the system size increases more than 50 times from 2048 to 108 000 atoms. Apparently, the size dependence is not as strong as the cooling rate dependence (figure 3(a)). Honeycutt and Andersen [49] argued that the use of periodic boundary conditions increases the nucleation rate in small systems (e.g. $N = 500$). This is because a crystal nucleus can easily overlap with its periodic images in small systems. In our smallest system ($N = 2048$), the box length is about 4.3 nm or 12.5 σ. At deep undercooling, the number of atoms in a critical nucleus is typically fewer than 100 or the nucleus radius is less than 3.0 σ. Thus, the distance between this nucleus and one of its periodic images is about 9.5 σ, which is much larger than the cutoff distance of the LJ potential

2.5 σ. This is why we did not see strong finite-size effects on the spontaneous crystallization temperature. Figure 4(b) shows the spontaneous crystallization temperature as a function of system size at the same cooling rate of 3.33×10^9 K s^{-1}. The spontaneous crystallization temperature scatters from 0.415 to 0.433 and the average temperature is 0.424. Therefore, the trend of the size dependence is not very clear. We believe these scattered datum points in figure 4(b) reflect the statistical nature of homogeneous nucleation, while the linear trend in figure 3(b) is caused by the cooling rate hysteresis.

5. Conclusions

In this work, we have used classical nucleation theory as a simple argument to compare the interfacial free energies calculated through different methods: primarily the planar-interface-based methods under equilibrium conditions and the curved-interface-based method under nonequilibrium conditions. Molecular dynamics simulations of freezing a pure liquid have been performed as independent tests to compare the spontaneous crystallization temperatures predicted by the theory. The finite-size effect and cooling rate effect in freezing simulations were carefully investigated to ensure the validity of the independent tests. We found that using the interfacial free energy obtained from the first method predicts nucleation rate several orders of magnitude lower than Turnbull's experimental results. Using the interfacial free energy calculated from the second method, the predicted nucleation rate is close to the experimental value. The possible causes for the discrepancy are discussed. The discrepancy in the interfacial free energies between the two methods is most likely caused by the curvature and temperature dependences of the interfacial free energy as well as the metastable interface structure at deep undercooling. Our results suggest that the crystal–melt interfacial free energy calculated from a planar interface needs to be adjusted to a smaller value in order to predict correct nucleation rate at deep undercooling.

Acknowledgments

The partial support of this work was provided by the Structural Amorphous Metals Program of DARPA under ARO contract no. DAAD19-01-1-0525 and Georgia Tech.

References

[1] Porter D A and Easterling K E 1992 *Phase Transformations in Metals and Alloys* (London: Chapman and Hall)
[2] Howe J M and Saka H 2004 *MRS Bull.* **29** 951–7
[3] Johnson E 2002 *Science* **296** 477–8
[4] Turnbull D 1952 *J. Chem. Phys.* **20** 411–24
[5] Turnbull D and Cech R E 1950 *J. Appl. Phys.* **21** 804–10
[6] Turnbull D 1950 *J. Appl. Phys.* **21** 1022–8
[7] Kelton K F, Greer A L, Herlach D M and Holland-Moritz D 2004 *MRS Bull.* **29** 940–4
[8] Broughton J Q and Gilmer G H 1986 *J. Chem. Phys.* **84** 5759–68
[9] Davidchack R L and Laird B B 2000 *Phys. Rev. Lett.* **85** 4751–4
[10] Davidchack R L and Laird B B 2003 *J. Chem. Phys.* **118** 7651–7
[11] Mu Y and Song X Y 2006 *J. Chem. Phys.* **124** 034712
[12] Hoyt J J, Asta M and Karma A 2001 *Phys. Rev. Lett.* **86** 5530–3
[13] Morris J R and Song X Y 2003 *J. Chem. Phys.* **119** 3920–5
[14] Bai X M and Li M 2005 *J. Chem. Phys.* **122** 224510
[15] Bai X M and Li M 2006 *J. Chem. Phys.* **124** 124707
[16] Sun D Y, Asta M and Hoyt J J 2004 *Phys. Rev.* B **69** 174103
[17] Davidchack R L, Morris J R and Laird B B 2006 *J. Chem. Phys.* **125** 094710
[18] Feng X B and Laird B B 2006 *J. Chem. Phys.* **124** 044707
[19] Bai X M and Li M 2007 *APS March Meeting (Denver, CO)* (abstract # K1.00136)
[20] Bai X M 2006 Thermodynamics and kinetics of phase transitions during supercooling and superheating: a theoretical and computational investigation in model Lennard-Jones systems *PhD Thesis* Georgia Institute of Technology
[21] Auer S and Frenkel D 2001 *Nature* **409** 1020–3
[22] Gasser U, Weeks E R, Schofield A, Pusey P N and Weitz D A 2001 *Science* **292** 258–62
[23] Trudu F, Donadio D and Parrinello M 2006 *Phys. Rev. Lett.* **97** 105701
[24] Leyssale J M, Delhommelle J and Millot C 2007 *J. Chem. Phys.* **127** 044504
[25] Delogu F 2008 *Nanotechnology* **19** 175703
[26] Davidchack R L and Laird B B 2005 *Phys. Rev. Lett.* **94** 086102
[27] Turnbull D 1969 *Contemp. Phys.* **10** 473–88
[28] Baez L A and Clancy P 1995 *J. Chem. Phys.* **102** 8138–48
[29] Aga R S, Morris J R, Hoyt J J and Mendelev M 2006 *Phys. Rev. Lett.* **96** 245701
[30] Shi G, Seinfeld J H and Okuyama K 1990 *Phys. Rev.* A **41** 2101–8
[31] Parrinello M and Rahman A 1981 *J. Appl. Phys.* **52** 7182–90
[32] Evans D J 1983 *J. Chem. Phys.* **78** 3297–302
[33] Allen M P and Tildesley D J 1987 *Computer Simulation of Liquids* (Oxford: Clarendon)
[34] Ostwald W Z 1897 *Z. Phys. Chem.* **22** 289–330
[35] ten Wolde P R, Ruizmontero M J and Frenkel D 1995 *Phys. Rev. Lett.* **75** 2714–7
[36] Leyssale J M, Delhommelle J and Millot C 2004 *J. Am. Chem. Soc.* **126** 12286–7
[37] Notthoff C, Feuerbacher B, Franz H, Herlach D M and Holland-Moritz D 2001 *Phys. Rev. Lett.* **86** 1038–41
[38] Shen Y C and Oxtoby D W 1996 *J. Chem. Phys.* **104** 4233–42
[39] Spaepen F and Meyer R B 1976 *Scr. Metall.* **10** 257–63
[40] Klein W and Leyvraz F 1986 *Phys. Rev. Lett.* **57** 2845–8
[41] Wang H, Gould H and Klein W 2007 *Phys. Rev.* E **76** 031604
[42] Wang H, Barros K, Gould H and Klein W 2007 *Phys. Rev.* E **76** 041116
[43] Spaepen F 1994 *Solid State Physics* (New York: Academic) pp 1–32
[44] Spaepen F 1994 *Mater. Sci. Eng.* A **178** 15–8
[45] Herhold A B, King H E and Sirota E B 2002 *J. Chem. Phys.* **116** 9036–50
[46] Tolman R C 1949 *J. Chem. Phys.* **17** 333
[47] Kashchiev D 2000 *Nucleation: Basic Theory with Applications* (Oxford: Butterworth Heinemann)
[48] Bai X M and Li M 2006 *Nano Lett.* **6** 2284–9
[49] Honeycutt J D and Andersen H C 1986 *J. Phys. Chem.* **90** 1585–9